

THE OUTER LIMITS OF THE M31 SYSTEM: KINEMATICS OF THE DWARF GALAXY SATELLITES AND XXVIII & AND XXIX*

ERIK J. TOLLERUD^{1,2,3}, MARLA C. GEHA¹, LUIS C. VARGAS¹, JAMES S. BULLOCK²*Draft version March 1, 2013*

ABSTRACT

We present Keck/DEIMOS spectroscopy of resolved stars in the M31 satellites And XXVIII & And XXIX. We show that these are likely self-bound galaxies based on 18 and 24 members in And XXVIII & And XXIX, respectively. And XXVIII has a systemic velocity of $-331.1 \pm 1.8 \text{ km s}^{-1}$ and velocity dispersion of $4.9 \pm 1.6 \text{ km s}^{-1}$, implying a mass-to-light ratio (within $r_{1/2}$) of $\sim 44 \pm 41$. And XXIX has a systemic velocity of $-194.4 \pm 1.5 \text{ km s}^{-1}$ and velocity dispersion of $5.7 \pm 1.2 \text{ km s}^{-1}$, implying a mass-to-light ratio (within $r_{1/2}$) of $\sim 124 \pm 72$. The internal kinematics and implied masses of And XXVIII & And XXIX are similar to dwarf spheroidals (dSphs) of comparable luminosities, implying that these objects are dark matter-dominated dwarf galaxies. Despite the large projected distances from their host (380 and 188 kpc), the kinematics of these dSph suggest that they are bound M31 satellites.

Subject headings: Local Group — galaxies: dwarf — galaxies: individual (And XXVIII, And XXIX, M31) — galaxies: kinematics and dynamics

1. INTRODUCTION

Local Group (LG) dwarf galaxies are crucial elements of near-field cosmology. They serve as valuable probes of low luminosity galaxy formation, and provide an important window into the nature of satellite-host interactions (e.g., Bullock et al. 2000; Strigari et al. 2007; Kravtsov 2010; Kazantzidis et al. 2011; Boylan-Kolchin et al. 2011; Anderhalden et al. 2012). Their utility stems primarily from their proximity and low surface densities, allowing spectroscopic observations of individual stars. This enables far more in-depth studies than are possible for more distant targets.

The numbers of known M31 and Milky Way (MW) dSph satellites has increased greatly in recent years. This is predominantly due to homogenous wide-field surveys, particularly the Sloan Digital Sky Survey (SDSS) for the MW (Willman et al. 2005; Belokurov et al. 2007), and the Pan-Andromeda Archeological Survey (PAndAS, Ibata et al. 2007; McConnachie et al. 2009). The environs of M31 have been particularly fertile ground for discovering dSphs, yielding 20 of its 28 known dSphs in the last six years.

Two of the most recently discovered M31 satellite candidates are And XXVIII, found by Slater et al. (2011), & And XXIX, by Bell et al. (2011). Projected in the plane of the sky at the distance of M31, And XXVIII & And XXIX lie at 380 and 188 kpc, respectively. The 3D distances from M31 are 367 and 188 kpc, using the tip

of the red giant branch (TRGB) line-of-sight distances of Slater et al. (2011) and Bell et al. (2011). The expected virial radius for M31's dark matter halo is $\sim 300 \text{ kpc}$ (Klypin et al. 2002; Watkins et al. 2010), so And XXIX lies in the outskirts of M31's halo and And XXVIII just outside. This makes And XXVIII the second-most distant M31 dSph⁵ satellite, with only And XVIII more distant (see §3.3).

And XXVIII, in particular, is potentially an important data point for galaxy formation. It may be an analog of Leo T, a satellite in the outskirts of the MW halo and the only low-luminosity MW satellite known to contain HI gas (Irwin et al. 2007; Ryan-Weber et al. 2008). This motivates more detailed studies of these M31 satellites, as Leo T has been valuable for understanding star formation and gas stripping in dSphs (e.g., Ricotti 2009; Grcevich & Putman 2009; Bovill & Ricotti 2011; Nichols & Bland-Hawthorn 2011). If they have no recent star formation, And XXVIII & And XXIX may be more akin to Tucana and Cetus. These are unusual, non-starforming dSphs of the LG that do not seem to be satellites (Lavery & Mighell 1992; Whiting et al. 1999; Monelli et al. 2010), but may be “backsplash” galaxies that were once much closer to either M31 or the MW (Knebe et al. 2011; Oman et al. 2013).

Here we present the first spectroscopic observations of And XXVIII & And XXIX, obtaining kinematics of resolved stars using the DEIMOS spectrograph on the Keck II Telescope. In §2, we describe our observations and analysis procedures, in §3 we present our kinematical measurements for And XXVIII & And XXIX, and in §4 we summarize and conclude. Throughout this paper we adopt a distance modulus to M31 of $\mu_{\text{M31}} = 24.47$, corresponding to a distance of 783 kpc (McConnachie et al. 2005), and distances of 650^{+150}_{-80} ($\mu = 24.06^{+0.5}_{-0.2}$) and $730 \pm 75 \text{ kpc}$ ($\mu = 24.31 \pm 0.22$) for And XXVIII &

¹ Astronomy Department, Yale University, P.O. Box 208101, New Haven, CT 06510, USA; erik.tollerud@yale.edu, marla.geha@yale.edu, luis.vargas@yale.edu

² Department of Physics and Astronomy, 4129 Frederick Reines Hall, University of California, Irvine, Irvine, CA, 92697, USA; bullock@uci.edu

³ Hubble Fellow

* The data presented herein were obtained at the W.M. Keck Observatory, which is operated as a scientific partnership among the California Institute of Technology, the University of California and the National Aeronautics and Space Administration. The Observatory was made possible by the generous financial support of the W.M. Keck Foundation

⁵ The starforming dIrrs IC1613 and Peg are more distant and possibly associated with M31 (McConnachie 2012).

And XXIX, respectively (Slater et al. 2011; Bell et al. 2011).

2. OBSERVATIONS AND ANALYSIS

2.1. Target Selection and Reduction

We selected stars for spectroscopic follow-up from the SDSS Data Release 8 photometric catalogs (Aihara et al. 2011). We selected stars near And XXVIII & And XXIX, eliminating objects where the SDSS *model* and *psf* magnitudes were discrepant by more than 0.25 mags. We then selected candidate dSph stars near the red giant branch (RGB) of a fiducial isochrone in the $g-i, r$ color-magnitude diagram (CMD). We used 12 Gyr Dartmouth isochrones (Dotter et al. 2008) offset by Schlegel et al. (1998) extinctions with $[\text{Fe}/\text{H}]$ and distance modulus matched to And XXVIII & And XXIX (Slater et al. 2011; Bell et al. 2011). We then populated the slitmask by selecting stars in the following sequence, prioritizing brighter stars for each group: those within 0.3 mags of the isochrone, those within 0.6 mags, and all remaining stars. The resulting selections covered a wide enough area in the CMD that our results do not depend strongly on the assumed distances and $[\text{Fe}/\text{H}]$ from Slater et al. (2011) and Bell et al. (2011).

2.2. Observations and Reduction

Spectroscopic observations were obtained on the nights of April 22–23 and September 16–17, 2012 using the DEIMOS spectrograph on the Keck II telescope (Faber et al. 2003). We used the 1200 lines mm^{-1} grating covering a wavelength region of 6400–9100 Å. This provided a FWHM resolution of ≈ 1.3 Å, equivalent to 50 km s^{-1} at the center of our wavelength range. We observed 3 slitmasks for And XXVIII, and 2 slitmasks for And XXIX, with an average exposure time of 3200 sec per mask.

Our spectroscopic reductions closely follow the procedure outlined in Tollerud et al. (2012). We reduce the spectra using the spec2d pipeline developed for the DEEP2 survey, which produces 1d spectra from the raw images (Davis et al. 2003; Cooper et al. 2012; Newman et al. 2012). In Figure 1, we show smoothed co-adds of the resulting spectra for members stars of And XXVIII & And XXIX (see §2.3 and 3 for membership determination). The average signal-to-noise ratio for these spectra was 4.8 per pixel.

We cross-correlate these 1d spectra with a series of high signal-to-noise ratio (SNR) templates of known radial velocity to determine a line-of-sight velocity. We determine errors on these velocities by re-simulating each spectrum 1000 times with noise added to simulate the per-pixel variance. We measure a cross-correlation velocity for each re-simulation, and use the mean and standard deviation of the distribution of velocities as the line-of-sight velocity and uncertainty for each star (Simon & Geha 2007). We also add in quadrature a systematic floor to the uncertainty, determined by repeat measurements of stars from Simon & Geha (2007), Kalirai et al. (2010), and Tollerud et al. (2012). These each found consistent values of of 2.2 km s^{-1} for the systematic floor over a temporal baseline longer than the time from these observations to Tollerud et al. (2012). Hence, we apply this same floor to the measurements in this work.

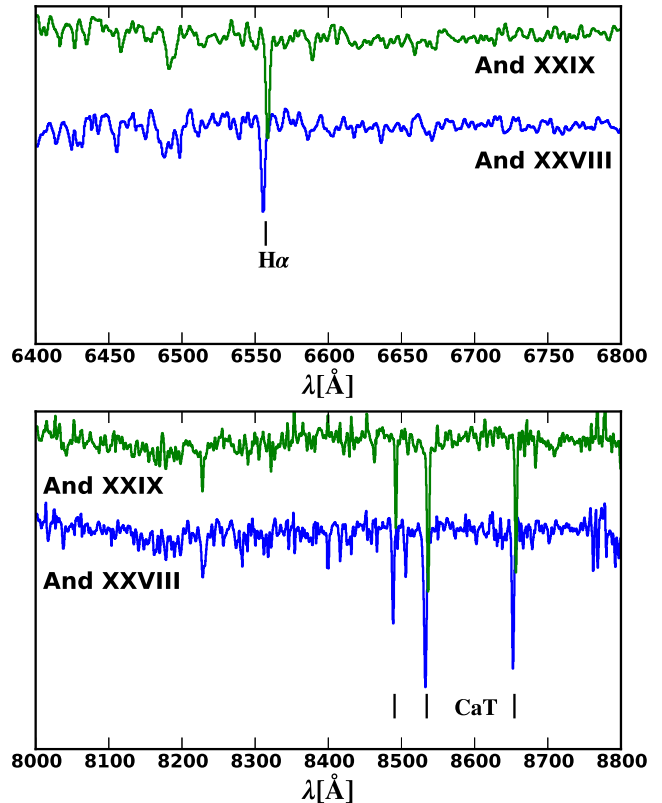


Figure 1. Continuum-normalized spectra of And XXVIII & And XXIX member stars. These spectra are inverse variance weighted heliocentric frame co-adds of 18 and 24 stars for And XXVIII & And XXIX, respectively, and have been smoothed with a 3-pixel gaussian filter for clarity. The lower (blue) line is for And XXVIII, while the upper (green) line is And XXIX. The top panel is a zoom near $\text{H}\alpha$, while the lower panel is a window that includes the calcium triplet (CaT). See §2.3 and 3 for details of membership determination. The vertical black lines marking $\text{H}\alpha$ and the CaT are at wavelengths where the features would be for a velocity halfway between the v_{sys} of And XXVIII & And XXIX. The offsets of the features in the spectra from these wavelengths are due to the differing v_{sys} of the dSphs.

2.3. Membership

A clean sample of member stars is crucial for determining the internal kinematics of And XXVIII & And XXIX. The two main sources of contamination for these observations are foreground MW stars and M31 halo stars. As demonstrated below, the MW foreground star velocity distribution is disjoint from the dSphs in the direction of And XXVIII & And XXIX, and hence the MW contaminants can mostly be filtered with velocity cuts. And XXVIII & And XXIX are far from M31 in projection (~ 380 and ~ 190 kpc projected, respectively), and thus the M31 halo dominates over the bulge or disk component (Courteau et al. 2011; Gilbert et al. 2012). We demonstrate in §2.4 that even the M31 halo density is low enough that its contamination is unlikely to affect our kinematic results for And XXVIII & And XXIX.

For both And XXVIII & And XXIX, our membership determination begins by selecting stars in the $r-i, r$ CMD. We select stars in a CMD box that encompasses stars near PARSEC isochrones (Bressan et al. 2012) for a 12 Gyr population with $[\text{Fe}/\text{H}]$ values that match the estimates from Slater et al. (2011) and Bell et al. (2011).

Table 1
Photometric and Kinematic Properties of And 28 & And 29

Row	Quantity	Units	And XXVIII	And XXIX
(1)	α (J2000)	h : m : s	22 ^h 32 ^m 41 ^s .2	23 ^h 58 ^m 55 ^s .6
(2)	δ (J2000)	° : ' : ''	31° 12' 58.2''	30° 45' 20.0''
(3)	d_{LOS}	kpc	650 ⁺¹⁵⁰ ₋₈₀	730 ± 75
(4)	M_V	mag	-8.5 ^{+0.4} _{-1.0}	-8.3 ± 0.4
(5)	R_{eff}	arcmin	1.11 ± 0.21	1.7 ± 0.2
(6)	R_{eff}	pc	210 ⁺⁶⁰ ₋₅₀	360 ± 60
(7)	[Fe/H]	dex	~ -2.0	~ -1.8
(8)	$r_{1/2}$	pc	280 ⁺⁸⁰ ₋₆₇	480 ± 80
Keck/DEIMOS Results				
(9)	N_{member}		18	24
(10)	v_{sys}	km s ⁻¹	-331.1 ± 1.8	-194.4 ± 1.5
(11)	σ_{LOS}	km s ⁻¹	4.9 ± 1.6	5.7 ± 1.2
(12)	$M/L_V (< r_{1/2})$	M_{\odot}/L_{\odot}	44 ± 41	124 ± 72
(13)	$M_{1/2}$	$M_{\odot} \times 10^6$	4.7 ± 3.2	11.1 ± 4.9

Note. — (1-7) Right ascension, declination, line-of-sight distance, absolute magnitude, effective radii, and metallicity are taken from Slater et al. (2011) and Bell et al. (2011) for And 28 & And 29, respectively.

These boxes are shown in the upper-left panels of Figures 2 and 3. We place the upper edge of these boxes above the tip of the isochrone because this accepts TRGB stars even if the And XXVIII & And XXIX distance moduli are $\sim 1\sigma$ off. To filter out the MW foreground stars that lie near the dSph members in the CMD, we impose a velocity window centered on the “cold spikes” apparent in the lower-left panels of Figures 2 and 3. The stars within these peaks and inside the CMD box are spatially concentrated near the centers of And XXVIII & And XXIX, as expected for a self-bound galaxy. Additionally, the absence of stars near these velocities above the TRGB of our chosen isochrones show even 2σ errors in the distances to And XXVIII & And XXIX would have no effect on our membership determination.

The velocity distributions of these candidate members are consistent with a Gaussian in the sense that both the Shapiro & Wilk (1965) and Anderson & Darling (1952) tests cannot reject the null hypothesis of Gaussianity at the $p = 0.05$ level. While these Gaussian peaks imply that most of the selected stars are members, we cannot discount the possibility of a small number of contaminants that by chance are near the dSph locus in both the CMD and velocity. To address this, we estimate the surface density of MW foreground stars expected in our spectroscopic sample using the Besançon model of the MW (Robin et al. 2003). We select model stars in the direction of each dSph which fall within the range of our observations in the $r - i$, r CMD. We then normalize the resulting model population such that the overall number of stars in the model match our observations for $v_{\text{helio}} > -100$ km s⁻¹, far from the dSph velocity. Finally, we determine how many stars in the model would fall within the velocity window for the dSph members. For both And XXVIII & And XXIX this number is small, ~ 0.7 and ~ 0.8 , respectively, in the entire field of our observations.

2.4. Kinematical Parameters

With a member sample selected as described above, we proceed to determine the internal kinematics of And XXVIII & And XXIX. In the sections below, we

model the velocity distribution of the member stars as a Gaussian with mean v_{sys} (systemic velocity), and dispersion σ_{LOS} . We determine the kinematical parameters of this model with a maximum likelihood fit, weighting all members equally, and use the inverse of the Hessian matrix to estimate the uncertainties on these parameters (Walker et al. 2007; Tollerud et al. 2012). We examine the resulting likelihood maps for v_{sys} and σ_{LOS} , and note that they are very close to Gaussian within 1σ of the peak. This validates the use of the Hessian matrix for estimating uncertainties, as it implicitly assumes the likelihood function near the maximum likelihood peak is approximately normal.

This approach assumes each star is only a tracer of the internal kinematics of the galaxy, and hence does not account for the impact of binary stars. As detailed in Minor et al. (2010) and McConnachie & Côté (2010), unresolved binaries can inflate the internal velocity dispersions measured for dSphs. Repeat velocity measurements are required to provide any meaningful correction for this effect, and this is not available for our data set. However, the uncertainties we report for And XXVIII & And XXIX below are larger than the corrections that result from multi-epoch observations of MW dSphs (Minor et al. 2010; Martinez et al. 2011; Minor 2013). Hence, unless M31 dSphs have substantially different binary populations than MW dSphs, is it unlikely unresolved binaries would have a major effect on the results we present here.

We also estimate the M31 halo surface density near And XXVIII & And XXIX. We start by determining stellar luminosity functions from PARSEC isochrones for [Fe/H] = -0.5 and -1.5, a range that approximately samples the metallicity range of the M31 halo (Gilbert et al. 2012). We use these luminosity functions to determine how many stars bright enough to meet our spectroscopic survey limits ($r \lesssim 22.5$) are present for a given surface brightness. For each dSph we then determine the M31 halo surface brightness using the best-fit power law from Gilbert et al. (2012). Combining these surface brightness estimates with the luminosity function thus provides an estimate of the number of M31

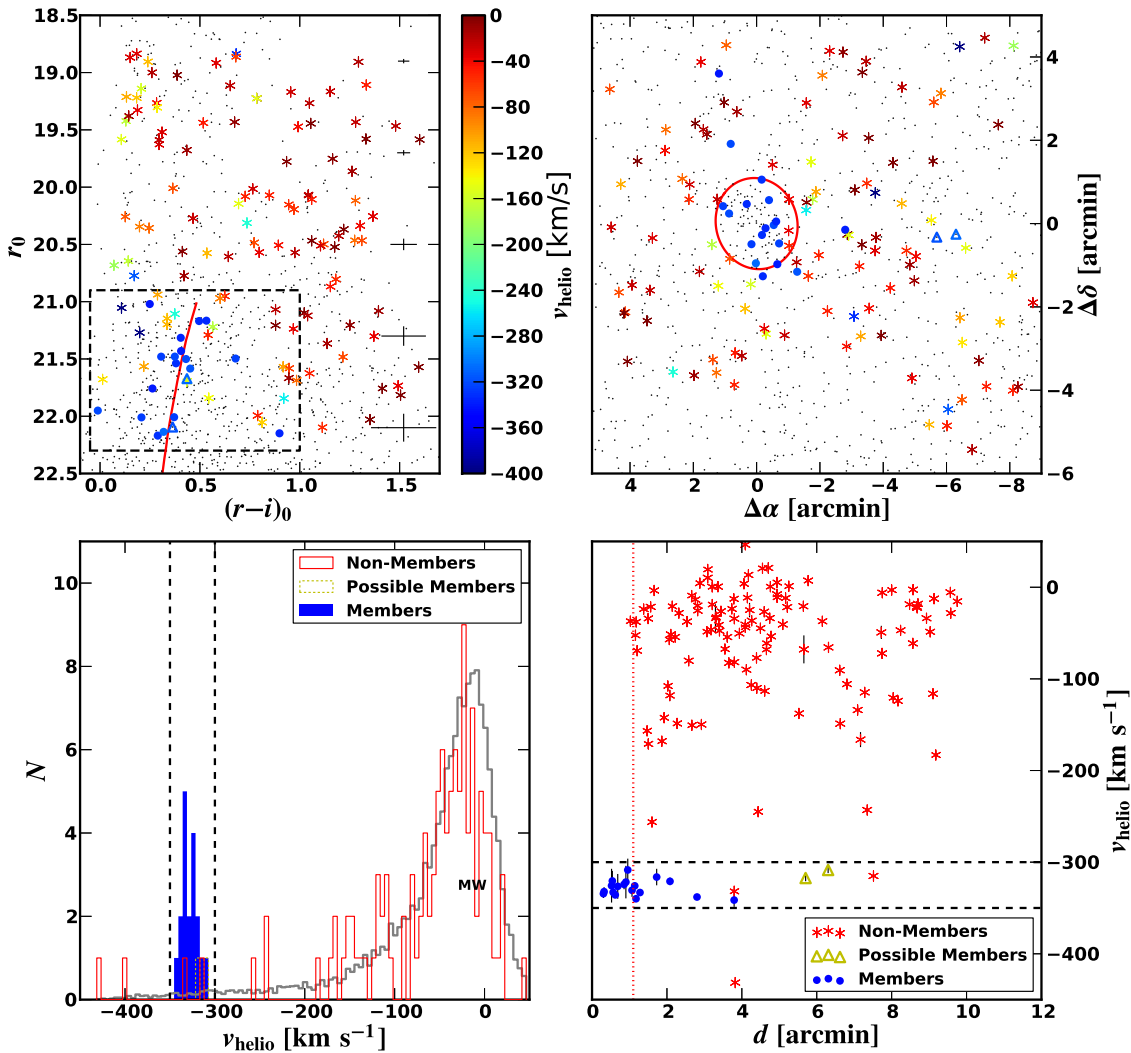


Figure 2. **Upper-left:** Foreground extinction-corrected r , $r-i$ CMD of the SDSS photometry of stars in the And XXVIII field. The points (black) are all star-like objects in the SDSS catalog in the spatial and CMD regions shown. Stars with spectroscopic data are colored by v_{helio} , with solid circles representing stars that are classified as members, outlined triangles are possible members (see text in §3.1), and asterisks are non-members. The (black) dashed box indicates the CMD selection window for membership, and the black error bars at $r-i=1.5$ are photometric errors in the SDSS averaged in magnitude bins. The solid (red) line is a PARSEC isochrone of 12 Gyr age and $[\text{Fe}/\text{H}] = -1.5$ (Bressan et al. 2012). **Upper-right:** Spatial Distribution of stars in the And XXVIII field. Symbols here are the same as those in the upper-left panel. The solid (red) line indicates the half-light ellipse. **Lower-left:** Velocity histogram for stars in the And XXVIII field. The blue histogram is member stars, while red is for non-members. The (black) dashed vertical lines indicate the velocity window used for membership. The gray line is the histogram of the Robin et al. (2003) model of MW foreground stars, normalized as described in §2.3. **Lower-right:** Radial velocity vs. distance from dSph in the And XXVIII field. Filled circles (blue) are members, outlined triangles (yellow) are the two stars of uncertain status, and star-shaped symbols (red) are non-members. Solid vertical lines are per-star velocity uncertainties. The (black) dashed line is the velocity window used for determining membership, while the (red) dotted line indicates the half-light radius of the dSph.

halo stars expected in our fields. We estimate ~ 0.3 M31 halo stars in our entire And XXVIII field, and ~ 2 M31 halo stars in our And XXIX observations. Furthermore, the M31 halo velocity distribution, while overlapping with the dSphs, is much hotter ($\sigma \sim 100 \text{ km s}^{-1}$, Chapman et al. 2006), further reducing the likelihood of an M31 halo star lying within our velocity window. While the predicted M31 halo and MW foreground contamination is small, we nonetheless simulate its effects in §3.4, showing that it should have no impact on our inferred kinematical results.

3. KINEMATIC RESULTS

3.1. And XXVIII

We present our observations of stars in the And XXVIII field in Figure 2. This object is far from M31 ($\sim 380 \text{ kpc}$ projected), but is relatively close to the Galactic plane ($b \sim -23^\circ$). There is a clear velocity peak at $v_{\text{sys}} \sim -300 \text{ km s}^{-1}$ (lower-right panel of Figure 2), well away from the velocity peak for MW stars ($v_{\text{helio}} \sim 0$). Applying our membership and kinematical analysis described in §2.3 and 2.4 (using a velocity window of -350 to -300 km s^{-1}) yields $v_{\text{sys}} = -328.0 \pm 2.3 \text{ km s}^{-1}$ and $\sigma_{\text{LOS}} = 8.1 \pm 1.8 \text{ km s}^{-1}$. Member stars are clustered near the photometric center (Upper-right panel

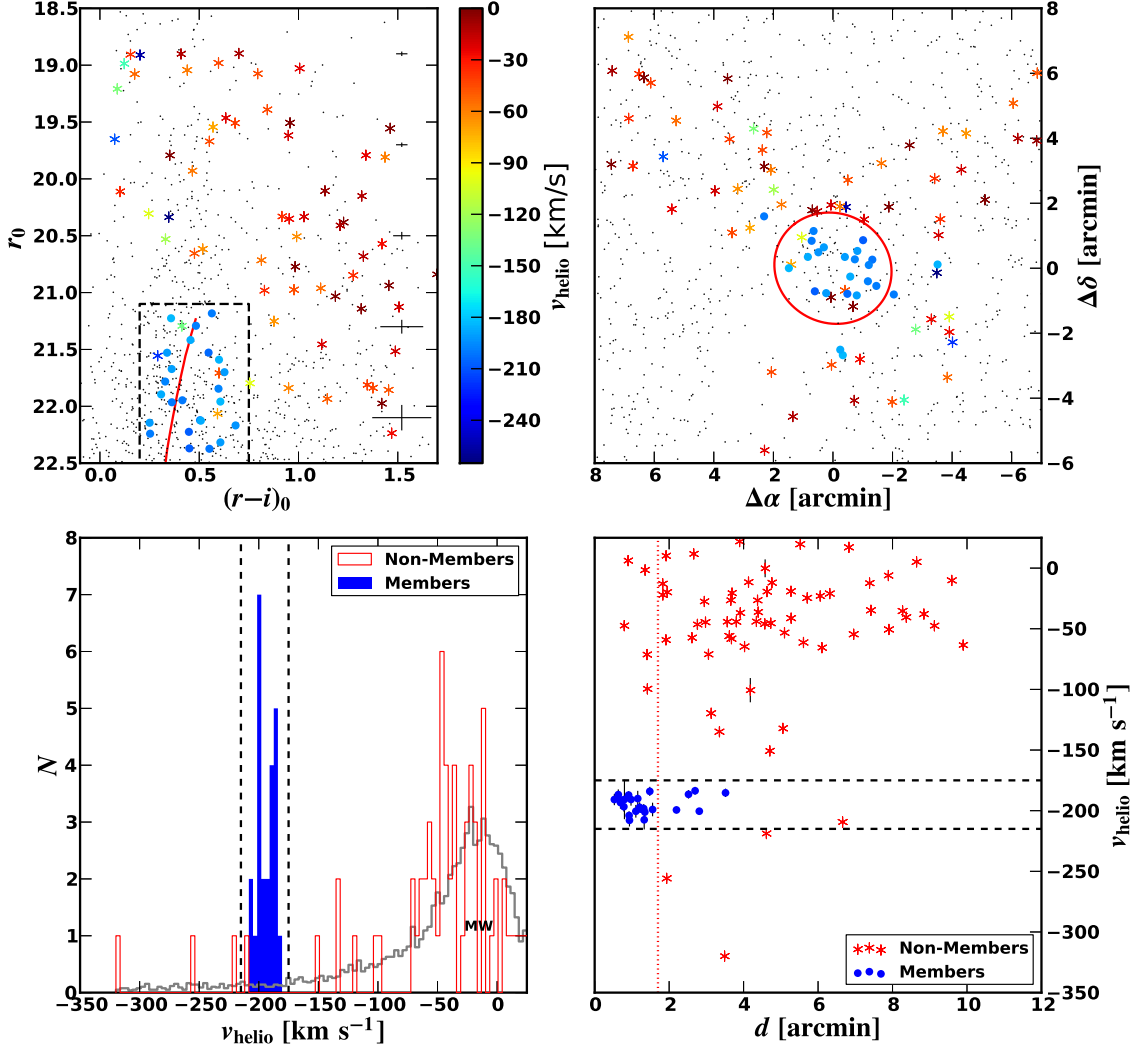


Figure 3. Same as Figure 2, but for And XXIX.

of Figure 2), and generally lie close to a fiducial isochrone for a dSph-like stellar population (Upper-right panel of Figure 2). While there are a few stars with velocities near the cold peak that appear to be outliers in the CMD, this is likely due to the relatively high photometric errors in this SDSS field.

The right panels of Figure 2 reveal two stars categorized as members that are at large distances from the photometric center of And XXVIII. Based on the analysis described in §2.3 (assuming the surface brightness profile from Slater et al. 2011), there should be no And XXVIII RGB stars at projected distances farther than these two stars (~ 1100 pc). These two stars are also velocity outliers. Thus, either And XXVIII’s surface brightness profile is intrinsically very different from other dSphs, the stars were tidally stripped, or these two stars are not associated with And XXVIII. Both stars’ spectra have an absorption equivalent width of ~ 0.7 Å for Na I $\lambda 8190$, a surface-gravity sensitive feature that is only detected in dwarf stars. This equivalent width marginally suggests they are dwarf stars, and hence unassociated foreground⁶. While the foreground star estimate from §2.3

suggests that two MW foregrounds are unlikely, Poisson statistics imply a probability of $\sim 5\%$, so it is possible that both stars are contaminants.

Hence, we also determine the kinematical parameters if these two stars are excluded, yielding $v_{\text{sys}} = -331.1 \pm 1.8$ km s $^{-1}$ and $\sigma_{\text{LOS}} = 4.9 \pm 1.6$ km s $^{-1}$. σ_{LOS} in this case is significantly smaller than if these stars are included, but is stable within 1σ to the exclusion of any other two stars. In the hypothesis that these stars are not members, this velocity dispersion provides an estimate of And XXVIII’s mass (see §3.5 for details). We combine this mass with the 3D distance from M31 (367 kpc) and a mass for M31 of $2 \times 10^{12} M_{\odot}$ (intentionally in the high range of M31 masses) to estimate the Jacobi tidal radius of And XXVIII (Binney & Tremaine 2008).

We find a tidal radius for And XXVIII of ~ 3.4 kpc, an order of magnitude larger than the current stellar extent ($R_e = 0.21$ kpc). This strongly supports the hypothesis that the two outlier stars were *not* recently stripped. Further, the v_{sys} measured here for And XXVIII is very close to the M31 v_{sys} . This may imply that it is near apocenter in its orbit, and thus is moving slowly (e.g., by a sky line.

⁶ For one of these stars the measurement may be contaminated

Boylan-Kolchin et al. 2012). Hence, stars stripped at pericenter should be far from And XXVIII. Taken together, this suggests And XXVIII has not recently been tidally stripped, and the two anomalous stars are contaminants. For our fiducial kinematic measurements of And XXVIII (listed in Table 1), we exclude these two stars as likely contaminants.

In either case, as described below in §3.5, this dispersion implies a mass-to-light ratio larger than any plausible stellar population. Hence, we confirm that And XXVIII is most likely a self-bound galaxy with a massive halo. Its status as a satellite of M31 is examined in detail in §3.3.

3.2. And XXIX

We present our spectroscopic measurements of stars in the And XXIX field along with the corresponding SDSS photometry in Figure 3. As in §3.1, a clear cold peak is present, but for And XXIX, the peak is closer to the MW peak at $v_{\text{helio}} \sim -200 \text{ km s}^{-1}$. While And XXIX is closer to M31 than And XXVIII ($\sim 190 \text{ kpc}$ projected), it is more offset from M31’s v_{sys} , and is farther from the Galactic plane than And XXVIII ($b \sim -31 \text{ deg}$). Thus both the MW and M31 contamination for the And XXIX field is less than And XXVIII. Indeed, applying our membership methodology to the cold peak (using a velocity window of -215 to -175 km s^{-1}) provides the histogram shown in the lower-right panel of Figure 3. This is consistent with a Gaussian distribution and has no obvious velocity outliers at large distances. We measure its kinematical parameters as described in §2.4, determine $v_{\text{sys}} = -194.4 \pm 1.5 \text{ km s}^{-1}$ and $\sigma_{\text{LOS}} = 5.7 \pm 1.2 \text{ km s}^{-1}$, and tabulate those results in Table 1. As for And XXVIII, these kinematical parameters are similar to those of other M31 and MW dSphs. We conclude that And XXVIII is also a self-bound dSph satellite of M31.

3.3. M31 Satellites or Local Group Field?

Both And XXVIII & And XXIX are at relatively large projected distances from M31 of 380 and 190 kpc, respectively. By contrast, the majority of M31’s dSphs lie within 150 kpc projected. This large difference is primarily a selection effect caused by the angular extent of the PAndAS survey. Nevertheless, the large projected separation begs the question of whether or not And XXVIII & And XXIX are truly satellites of M31 rather than “free floating” galaxies of the LG (e.g., Tucana and Cetus). While the typical usage of the word “satellite” for these galaxies is sometimes ambiguous, here we define it to mean an object that is instantaneously bound to its host at the current epoch.

Figure 4 plots v_{sys} , the line-of-sight relative to M31, against the 3D distance from M31 for a selection of dSphs. Also shown (as green curves) are the one-dimensional escape velocity (i.e., $v_{\text{esc}}/\sqrt{3}$) for the M31 halo model of Klypin et al. (2002) ($M_{\text{vir}} = 1.6 \times 10^{12} M_{\odot}$). A satellite lying above this curve is thus unbound if its two tangential velocity components are equal to its observed line-of-sight v_{sys} . It is clear from inspection of this plot that both And XXVIII (blue circle) & And XXIX (red square) lie well within these curves, indicating that their tangential velocity components must

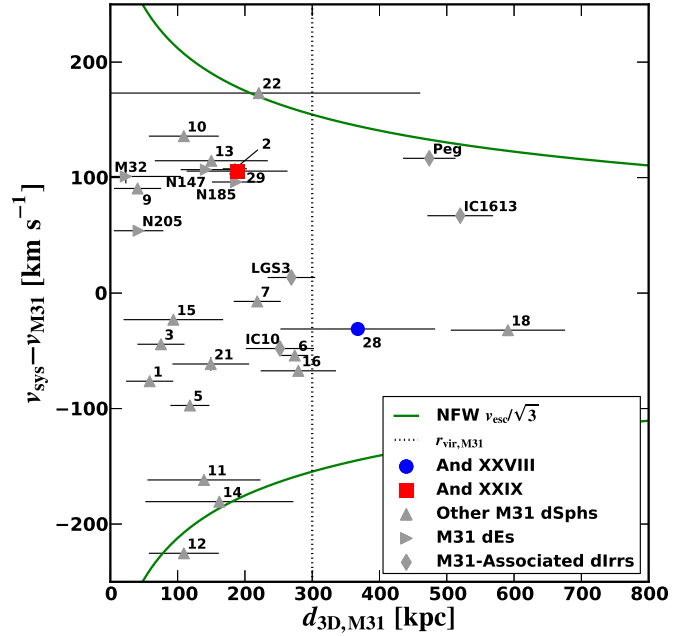


Figure 4. Distance vs. line-of-sight v_{sys} for M31-associated dwarf galaxies. The (blue) circle and (red) square are from this work, And XXVIII & And XXIX, respectively. Up-pointing triangles (gray) are dSphs from the samples of Collins et al. (2011), Tollerud et al. (2012) and Ho et al. (2012). Diamonds and right-pointing triangles (gray) are dIrrs and dEs from McConnachie (2012). The distance axis is 3D distance from M31, computed by combining the projected separation of the dSphs from M31 with line-of-sight TRGB distances. The (black) vertical dotted line is the virial radius of M31 from the Klypin et al. (2002) model. The (green) curves are the one-dimensional escape velocities from an NFW dark matter halo matching the model of Klypin et al. (2002). To make them one-dimensional, we divide the escape velocities by $\sqrt{3}$, so they represent the v_{sys} above which a satellite would be unbound if its (unmeasured) tangential velocity components were equal to v_{sys} . And XXVIII & And XXIX lie well within the bound region.

exceed the line-of-sight velocity by a large margin to not be bound to M31. This holds even for And XXVIII, despite the fact that it lies beyond M31’s virial radius (vertical dashed line in Figure 4).

Also of note in Figure 4 is the satellite status of the most distant dSph, And XVIII. Its v_{sys} is only $\sim 30 \text{ km s}^{-1}$ from M31, despite being nearly as far behind M31 as M31 is from the MW. While this strongly suggests it is formally bound to M31, the free-fall time for And XVIII to reach M31 is greater than the time in which M31 is likely to merge with the MW (van der Marel et al. 2012). Hence, systems as distant from M31 (or the MW) as And XVIII might be better considered satellites of the future merged M31/MW galaxy.

While the v_{sys} measurements for these galaxies are suggestive, they cannot definitively determine if a satellite is bound due to the unmeasured tangential velocity. However, the evidence that dark matter halos are present in both And XXVIII & And XXIX (§3.5) provides strong constraints. Boylan-Kolchin et al. (2012) shows that in Λ CDM simulations of either MW or M31-like halos, halos at distances from the host like those of And XXVIII or And XXIX are nearly always ($> 99.9\%$) bound. In a Λ CDM context, it is thus extremely likely that And XXVIII & And XXIX are M31 satellites.

3.4. Contamination Simulations

The method described in §2.4 for estimating kinematic parameters assumes a pure sample of dSph member stars and does not formally account for the possibility of contamination due to MW foregrounds and M31 halo stars (discussed in §2.3). To determine if such contamination might affect our kinematical results, we simulate the effect of contamination on our parameter estimates by creating mock velocity datasets designed to mimic And XXVIII & And XXIX.

For each dSph we create 10000 mock datasets composed of a Gaussian distribution with kinematic parameters corresponding to our results for the dSph. We add to this two additional uniform distributions with normalization set to match the number of expected stars in the MW foreground and M31 halo as estimated in §2.3. We account for fractional numbers of contaminants by only including an additional contaminant star for a corresponding fraction of the mock datasets. We then measure the kinematical parameters of these mock velocity distributions, and compare them to the input parameters used to generate the mock datasets.

We generate mock datasets based on both the And XXVIII & And XXIX fields following the prescription described above. For both sets of mocks, the estimated σ_{LOS} and v_{sys} were very close to the true value used to initialize the mock datasets. More specifically, the variance in the difference between the true and estimated values due to the contamination is $\sim 5\times$ lower than the variance in each measurement due to small number statistics. Thus, contamination at the level we estimate here cannot have a statistically significant impact on our results.

3.5. Mass Estimates

With reliable kinematical parameters in hand, we are now in a position to estimate the mass of these galaxies from their internal velocities. We search for rotation by dividing the galaxies in half and search for mean velocities of opposite sign on each side, over a range of position angles. We find that the maximal rotation signal for either galaxy is negligible relative to the dispersion, $< 1 \text{ km s}^{-1}$. Hence we model the galaxies as purely pressure-supported systems. We estimate the mass of these galaxies from their velocity dispersions ($M_{1/2}$) following Equation 2 of Wolf et al. (2010), and tabulate these for And XXVIII & And XXIX in Table 1. The mass obtained with this formula is not strongly degenerate with the anisotropy, but in this interpretation, it is only valid as a mass measurement within the deprojected (3D) half-light radius⁷. Applying this to our kinematical parameter estimates yields $M_{1/2}(< r_{1/2}) = 4.7 \pm 3.2 \times 10^6 M_{\odot}$ for And XXVIII, and $M_{1/2}(< r_{1/2}) = 1.1 \pm 0.49 \times 10^7 M_{\odot}$ for And XXIX.

A simple mass-to-light ratio estimate may be obtained by dividing this $M_{1/2}$ by the luminosity within $r_{1/2}$ – by definition this is $L/2$. For And XXVIII, we obtain $M/L_V(< r_{1/2}) = 44 \pm 41 M_{\odot}/L_{\odot}$, and for And XXIX, we find $M/L_V(< r_{1/2}) = 123 \pm 72 M_{\odot}/L_{\odot}$. Like other M31

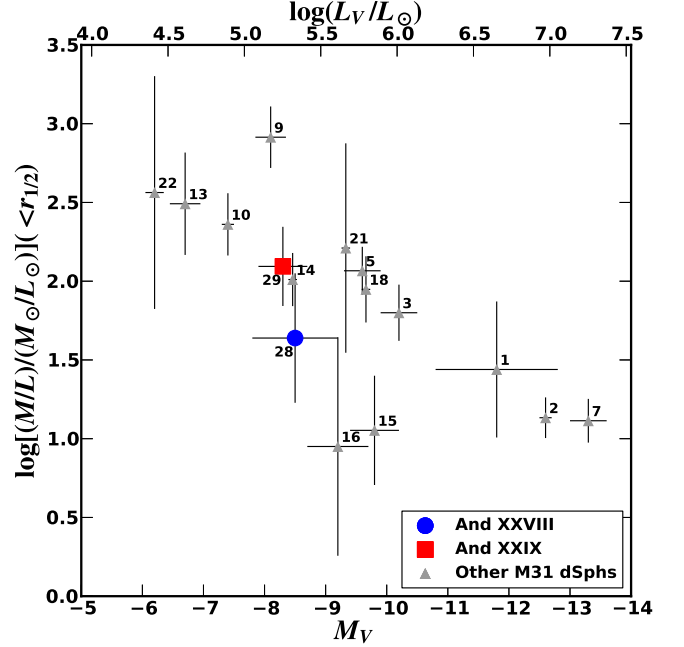


Figure 5. Log of Mass-to-light ratio vs. Luminosity for M31 dSphs. And XXVIII & And XXIX are represented as a (blue) circle and (red) square, while other M31 dSphs from Tollerud et al. (2012) and Ho et al. (2012) are (gray) triangles. Masses are determined using the Wolf et al. (2010) mass estimator (using half-light radii from Brasseur et al. 2011), which is valid when interpreted as the mass within the deprojected (3D) half-light radius. Both And XXVIII & And XXIX lie in the range of other M31 dSphs and have mass-to-light ratios greater than plausible from their stellar populations alone, implying they are dark matter-dominated.

dSphs of similar luminosity (see Figure 5), And XXVIII & And XXIX have mass-to-light ratios above those that are possible for purely stellar systems. This reveals the presence of a dark matter halo, even within the half-light radius, where baryons dominate for brighter galaxies (e.g., Strigari et al. 2008b,a; Walker et al. 2009; Tollerud et al. 2011). For And XXVIII, the uncertainty admits a stellar-like M/L at the 1σ level, primarily due to uncertainty in the galaxy’s luminosity, but the best estimate is well above any plausible stellar value. Alternatively, McGaugh & Milgrom (2013), under a Modified Newtonian Dynamics (MOND) hypothesis, have recently predicted velocity dispersions for And XXVIII & And XXIX of $4.3^{+0.8}_{-0.7}$ $4.1^{+0.8}_{-0.7} \text{ km s}^{-1}$ (error bars are from assuming mass-to-light ratios from 1 to $4 M_{\odot}/L_{\odot}$). These predictions are marginally consistent with our measurements, but whether this is numerical coincidence given the uncertainties or evidence for MOND is beyond the scope of this paper (Kaplinghat & Turner 2002; McGaugh 2011; Foreman & Scott 2012; Gnedin 2012).

In Figure 5, we show the mass-to-light ratios of And XXVIII & And XXIX in the context of other M31 dSphs. This plot demonstrates that their internal dynamics are fairly typical of M31’s dSphs, despite their distance from their host. This implies that the processes shaping these dSphs’ kinematic structure either operate quickly upon infall, are in place before the satellites interacted with M31, or both And XXVIII & And XXIX have been in the M31 system for some time and have already been influenced by M31’s environment (e.g., Wetzel et al. 2012). These trends are also similar to MW dSphs, sug-

⁷ For surface brightness profiles appropriate for dSphs, however, the deprojected (3D) half-light radius is well estimated as $4R_{\text{eff}}/3$ where R_{eff} is the projected half-light radius.

gesting these processes are not unique to the M31 system (Tollerud et al. 2012).

4. CONCLUSIONS

The spectroscopic observations of the And XXVIII & And XXIX fields described here support the following conclusions:

1. We have spectroscopically confirmed that And XXVIII & And XXIX are likely self-bound dwarf galaxies, with velocity dispersions of 4.9 ± 1.6 and 5.7 ± 1.2 km s⁻¹, respectively. The implied large mass-to-light ratios are consistent with dark matter-dominated dynamics.
2. While they are in the outskirts of the M31 system, the systemic velocities of And XXVIII & And XXIX imply they are both bound to M31.
3. The internal kinematics and implied masses of And XXVIII & And XXIX are like those of other dSphs of similar luminosities, despite the large distances from their host.

While these results clearly demonstrate that And XXVIII & And XXIX are self-bound dwarf satellites of M31, their nature and evolutionary history are still open questions. And XXIX seems to have only older (\gtrsim a few Gyr) stars (Bell et al. 2011), but And XXVIII's stellar population is less constrained by the SDSS photometry (Slater et al. 2011). The paucity of stars near And XXVIII with $g - r < 0$ or $r - i < 0$ implies it cannot have as much recent star formation as Leo T, but low levels of intermediate-age stars cannot be completely ruled out without deeper photometry. Further, without HI data, it cannot be definitively determined if these galaxies are truly passive dSphs, or a "transition"-type dSph/dIrr objects in a low star-formation episode.

The lack of recent star formation in And XXVIII is surprising, as it stands in contrast to galaxies at similar distances from their hosts like Leo T and the Phoenix Dwarf. Yet unlike Tucana and Cetus, And XXVIII is unambiguously associated with M31. Thus, And XXVIII stands as an important data point for understanding the evolutionary history of dSphs satellites and their connection to field galaxies.

The authors acknowledge Sarah Benjamin, Ana Bonaca, Nitya Kallivayalil, and Nhung Ho for valuable feedback on this manuscript. We also thank the referee (Alan McConnachie) for helpful feedback that improved this work.

Support for this work was provided by NASA through Hubble Fellowship grant #51316.01 awarded by the Space Telescope Science Institute, which is operated by the Association of Universities for Research in Astronomy, Inc., for NASA, under contract NAS 5-26555.

The authors wish to recognize and acknowledge the very significant cultural role and reverence that the summit of Mauna Kea has always had within the indigenous Hawaiian community. We are most fortunate to have the opportunity to conduct observations from this mountain.

Funding for SDSS-III has been provided by the Alfred P. Sloan Foundation, the Participating Institutions, the National Science Foundation, and the U.S. Department of Energy Office of Science. The SDSS-III web site is <http://www.sdss3.org/>.

SDSS-III is managed by the Astrophysical Research Consortium for the Participating Institutions of the SDSS-III Collaboration including the University of Arizona, the Brazilian Participation Group, Brookhaven National Laboratory, University of Cambridge, Carnegie Mellon University, University of Florida, the French Participation Group, the German Participation Group, Harvard University, the Instituto de Astrofísica de Canarias, the Michigan State/Notre Dame/JINA Participation Group, Johns Hopkins University, Lawrence Berkeley National Laboratory, Max Planck Institute for Extraterrestrial Physics, New Mexico State University, New York University, Ohio State University, Pennsylvania State University, University of Portsmouth, Princeton University, the Spanish Participation Group, University of Tokyo, University of Utah, Vanderbilt University, University of Virginia, University of Washington, and Yale University.

This research made use of Astropy (<http://www.astropy.org>), a community-developed core Python package for Astronomy.

Facilities: Keck:II (DEIMOS), APO (SDSS) And XXVIII, And XXIX, M31

REFERENCES

- Aihara, H., Allende Prieto, C., An, D., et al. 2011, *ApJS*, 193, 29
- Anderhalden, D., Schneider, A., Maccio, A. V., Diemand, J., & Bertone, G. 2012, *ArXiv e-prints*, arXiv:1212.2967, submitted to *JCAP*
- Anderson, T. W., & Darling, D. A. 1952, *The Annals of Mathematical Statistics*, 23, 193
- Bell, E. F., Slater, C. T., & Martin, N. F. 2011, *ApJ*, 742, L15
- Belokurov, V., Zucker, D. B., Evans, N. W., et al. 2007, *ApJ*, 654, 897
- Binney, J., & Tremaine, S. 2008, *Galactic Dynamics: Second Edition* (Princeton University Press)
- Bovill, M. S., & Ricotti, M. 2011, *ApJ*, 741, 18
- Boylan-Kolchin, M., Bullock, J. S., & Kaplinghat, M. 2011, *MNRAS*, 415, L40
- Boylan-Kolchin, M., Bullock, J. S., Sohn, S. T., Besla, G., & van der Marel, R. P. 2012, *ArXiv e-prints*, arXiv:1210.6046, submitted to *ApJ*
- Brasseur, C. M., Martin, N. F., Macciò, A. V., Rix, H.-W., & Kang, X. 2011, *ApJ*, 743, 179
- Bressan, A., Marigo, P., Girardi, L., et al. 2012, *MNRAS*, 427, 127
- Bullock, J. S., Kravtsov, A. V., & Weinberg, D. H. 2000, *ApJ*, 539, 517
- Chapman, S. C., Ibata, R., Lewis, G. F., et al. 2006, *ApJ*, 653, 255
- Collins, M. L. M., Chapman, S. C., Rich, R. M., et al. 2011, *MNRAS*, 417, 1170
- Cooper, M. C., Newman, J. A., Davis, M., Finkbeiner, D. P., & Gerke, B. F. 2012, in *Astrophysics Source Code Library*, record ascl:1203.003, 3003
- Courteau, S., Widrow, L. M., McDonald, M., et al. 2011, *ApJ*, 739, 20
- Davis, M., Faber, S. M., Newman, J., et al. 2003, in *Society of Photo-Optical Instrumentation Engineers (SPIE) Conference Series*, Vol. 4834, *Society of Photo-Optical Instrumentation Engineers (SPIE) Conference Series*, ed. P. Guhathakurta, 161–172
- Dotter, A., Chaboyer, B., Jevremović, D., et al. 2008, *ApJS*, 178, 89

- Faber, S. M., Phillips, A. C., Kibrick, R. I., et al. 2003, in Society of Photo-Optical Instrumentation Engineers (SPIE) Conference Series, Vol. 4841, Society of Photo-Optical Instrumentation Engineers (SPIE) Conference Series, ed. M. Iye & A. F. M. Moorwood, 1657–1669
- Foreman, S., & Scott, D. 2012, *Physical Review Letters*, 108, 141302
- Gilbert, K. M., Guhathakurta, P., Beaton, R. L., et al. 2012, *ApJ*, 760, 76
- Gnedin, N. Y. 2012, *ApJ*, 754, 113
- Grcevich, J., & Putman, M. E. 2009, *ApJ*, 696, 385
- Ho, N., Geha, M., Munoz, R. R., et al. 2012, *ApJ*, 758, 124
- Ibata, R., Martin, N. F., Irwin, M., et al. 2007, *ApJ*, 671, 1591
- Irwin, M. J., Belokurov, V., Evans, N. W., et al. 2007, *ApJ*, 656, L13
- Kalirai, J. S., Beaton, R. L., Geha, M. C., et al. 2010, *ApJ*, 711, 671
- Kaplinghat, M., & Turner, M. 2002, *ApJ*, 569, L19
- Kazantzidis, S., Lokas, E. L., Callegari, S., Mayer, L., & Moustakas, L. A. 2011, *ApJ*, 726, 98
- Klypin, A., Zhao, H., & Somerville, R. S. 2002, *ApJ*, 573, 597
- Knebe, A., Libeskind, N. I., Knollmann, S. R., et al. 2011, *MNRAS*, 412, 529
- Kravtsov, A. 2010, *Advances in Astronomy*, 2010, 281913
- Lavery, R. J., & Mighell, K. J. 1992, *AJ*, 103, 81
- Martinez, G. D., Minor, Q. E., Bullock, J., et al. 2011, *ApJ*, 738, 55
- McConnachie, A. W. 2012, *AJ*, 144, 4
- McConnachie, A. W., & Côté, P. 2010, *ApJ*, 722, L209
- McConnachie, A. W., Irwin, M. J., Ferguson, A. M. N., et al. 2005, *MNRAS*, 356, 979
- McConnachie, A. W., Irwin, M. J., Ibata, R. A., et al. 2009, *Nature*, 461, 66
- McGaugh, S. 2011, *ArXiv e-prints*, arXiv:1109.1599
- McGaugh, S., & Milgrom, M. 2013, *ArXiv e-prints*, arXiv:1301.0822
- Minor, Q. E. 2013, *ArXiv e-prints*, arXiv:1302.0302
- Minor, Q. E., Martinez, G., Bullock, J., Kaplinghat, M., & Trainor, R. 2010, *ApJ*, 721, 1142
- Monelli, M., Gallart, C., Hidalgo, S. L., et al. 2010, *ApJ*, 722, 1864
- Newman, J. A., Cooper, M. C., Davis, M., et al. 2012, *ArXiv e-prints*, arXiv:1203.3192
- Nichols, M., & Bland-Hawthorn, J. 2011, *ApJ*, 732, 17
- Oman, K. A., Hudson, M. J., & Behroozi, P. S. 2013, *ArXiv e-prints*, arXiv:1301.6757
- Ricotti, M. 2009, *MNRAS*, 392, L45
- Robin, A. C., Reylé, C., Derrière, S., & Picaud, S. 2003, *A&A*, 409, 523
- Ryan-Weber, E. V., Begum, A., Oosterloo, T., et al. 2008, *MNRAS*, 384, 535
- Schlegel, D. J., Finkbeiner, D. P., & Davis, M. 1998, *ApJ*, 500, 525
- Shapiro, S. S., & Wilk, M. B. 1965, *Biometrika*, 52, 591
- Simon, J. D., & Geha, M. 2007, *ApJ*, 670, 313
- Slater, C. T., Bell, E. F., & Martin, N. F. 2011, *ApJ*, 742, L14
- Strigari, L. E., Bullock, J. S., Kaplinghat, M., et al. 2008a, *Nature*, 454, 1096
- Strigari, L. E., Koushiappas, S. M., Bullock, J. S., & Kaplinghat, M. 2007, *Phys. Rev. D*, 75, 083526
- Strigari, L. E., Koushiappas, S. M., Bullock, J. S., et al. 2008b, *ApJ*, 678, 614
- Tollerud, E. J., Bullock, J. S., Graves, G. J., & Wolf, J. 2011, *ApJ*, 726, 108
- Tollerud, E. J., Beaton, R. L., Geha, M. C., et al. 2012, *ApJ*, 752, 45
- van der Marel, R. P., Besla, G., Cox, T. J., Sohn, S. T., & Anderson, J. 2012, *ApJ*, 753, 9
- Walker, M. G., Mateo, M., Olszewski, E. W., et al. 2007, *ApJ*, 667, L53
- . 2009, *ApJ*, 704, 1274
- Watkins, L. L., Evans, N. W., & An, J. H. 2010, *MNRAS*, 406, 264
- Wetzell, A. R., Tinker, J. L., & Conroy, C. 2012, *MNRAS*, 424, 232
- Whiting, A. B., Hau, G. K. T., & Irwin, M. 1999, *AJ*, 118, 2767
- Willman, B., Dalcanton, J. J., Martinez-Delgado, D., et al. 2005, *ApJ*, 626, L85
- Wolf, J., Martinez, G. D., Bullock, J. S., et al. 2010, *MNRAS*, 406, 1220